Proceedings World Geothermal Congress 2020+1
Reykjavik, Iceland, April - October 2021

Reactive Reservoir Systems – Crystal Nucleation and Filter Processes in Geothermal Systems

Philipp Zuber, Sascha Frank, Jürgen Schreuer and Stefan Wohnlich

Ruhr-University Bochum, Universitätsstraße 150, D-44801 Bochum, Germany

philipp.zuber@rub.de

Keywords: barite, scaling, crystal nucleation, morphology, filter processes

ABSTRACT

During geothermal energy generation, the change of temperature and pressure conditions can lead to supersaturation in the extracted fluids and therefore to the precipitation of crystalline phases. Well-documented crystalline deposits on the inner walls of pipes are the consequences. In addition, turbulence-induced inhomogeneities and mechanical disturbances also lead to the spontaneous formation of free-floating crystal nuclei. A significant part of them are carried along and reinjected into the reservoir. There, the crystal nuclei are possible centers for crystallization and cementations processes or can accumulate by filter effects. Both processes contribute to scaling effects which limit the permeability of the geothermal reservoir and therefore the profitability of a geothermal installation. So far, such effects have been barely considered in previous studies.

Our investigations focus on a better understanding of the formation and growth of crystal nuclei in saturated geothermal solutions during thermal and pressure relaxation, and their role in decreasing permeability of fractured geothermal reservoirs. For this purpose, a high-pressure-high-temperature apparatus which is based on the working principle of a geothermal cycle was built and used. Circulating flow-through experiments with fractured reservoir rocks and barite-supersaturated fluids are conducted under geothermal conditions with the option to simulate heat extraction and injection of colder crystal-contaminated fluids. Furthermore, the size and morphology of precipitated barite crystals are studied as important factors influencing the potential filter processes in fractures. First results show substantial change in barite morphology with different sodium chloride concentrations in solution. To minimize the scaling effects, the goal is to develop approaches to control crystal nucleation.

1. INTRODUCTION

The profitability of a geothermal installation is dependent on high flow rates and therefore high permeability of the reservoir rock. Permeability in geothermal systems is mainly supported by fracture zones and not by porous matrix as fracture permeability exceeds matrix permeability (Vidal and Genter, 2018). During a geothermal production cycle, a fluid is produced, the heat is extracted, and the cooled fluid is reinjected through injection wells into the reservoir where it can be heated again and circulate back to the production wells through fractures. However, examples show that the decrease of permeability in fractured reservoirs is a serious threat to the long-term use of geothermal resources and requires cost-intensive measures, e. g. hydraulic or chemical stimulation (Blöcher et al., 2016).

The change of temperature and pressure conditions during heat extraction leads to a change of the chemical equilibrium and can therefore lead to a supersaturation and precipitation of crystalline phases (scales). The fluid composition and the degree of temperature and pressure reduction determine the phases precipitating. The main phases are carbonates ($CaCO_3$), sulfates ($CaSO_4$, $BaSO_4$, $SrSO_4$), silica (SiO_2), and sulfides (FeS, PbS, CuS) (Stober and Bucher, 2014). As a result, these phases are primally deposited on the inner walls of heat exchangers, pipes and even the inner casing of injection wells, reducing the efficiency of the installation (Bott, 1995; Scheiber et al., 2013). These scaling processes are already well-documented for many geothermal systems (Wolfgramm et al., 2011).

In addition to the deposits on inner walls, turbulence-induced inhomogeneities and mechanical disturbances lead to homogeneous nucleation of free-floating crystallites. A significant part of them are carried along and reinjected into the reservoir. There, the crystal nuclei are possible centers for crystallization and cementations processes or can accumulate by filter effects. These effects change considerably with different crystal morphologies as the clogging behavior increases from isometric to lamellar and acicular crystal habits.

A high-pressure-high-temperature apparatus was developed and built to simulate a geothermal cycle and its scaling processes. An artificial fluid is circulated under geothermal conditions through a water reservoir autoclave, a heat exchanger and a sample autoclave which holds a fractured cylindrical rock sample. The fluid is preconditioned regarding to the used sample to minimize mineral dissolution during flow-through. Furthermore, the used fluid is saturated with a mineral phase to force precipitation during cooling in the heat exchanger. The fluid and precipitated crystallites are then led into the sample autoclave in front of the fractured core. Additionally, it's possible to inject suspensions into the system containing specific crystal seeds with different morphologies through a high-pressure pump to study the filter effects of different crystal habits.

This study focuses on barite precipitations in fractured Flechtinger sandstone. The Flechtinger sandstone is an analogous rock for the reservoir at Groß-Schönebeck (Germany) which is known for barite scalings in the surface installations (Scheiber et al., 2014; Regenspurg et al., 2015). Complementary laboratory experiments are conducted to study the size and morphology of barite crystals precipitated from artificial geothermal fluids.

2. METHODS

2.1 Precipitation Experiments

To be able to produce crystallites with specific crystal morphologies it is necessary to study crystal growth as a function of temperature, time and concentrations of solutes (e. g. Na, K, Ca, Mg, Sr, Ba, Cl, SO_4). For this reason, precipitation experiments were conducted. One method to force precipitation is to produce a supersaturation by mixing of two solutions (fig. 1). In each case barium chloride dihydrate (Riedel-de Haën AG, 99 %) and sodium sulfate decahydrate (VWR Chemicals, 99.9 %) were solved in pure water (type II), stirred for 5 minutes and mixed. The solids were separated from the resulting suspension by vacuum filtration with 0.45 and 0.10 µm cellulose nitrate filter membranes (Sartorius AG), rinsed with pure water and dried.

Different concentrations of Ba and SO_4 were used (0.4, 0.3, 0.4, 0.5, 0.6, 0.7, 0.8, 0.9, 1.0 and 2.0 mmol/L) and the duration after mixing of the two solutions was varied (10, 30, 60 s; 2, 3, 5, 10, 20, 60 min and 5, 15, 30 h). Some precipitation experiments were conducted at elevated temperatures (60 and 90 °C). The main investigations were carried out to study the influence of sodium chloride (0 to 5 mol/L; Fisher Chemical, 99.5 %) and diethylenetriaminepentakis (methylphosphonic acid) (DTPMP; Sigma-Aldrich, technical solution: ~ 50% (T), H_2O ~ 35 %, HCl 15 %) in solution.

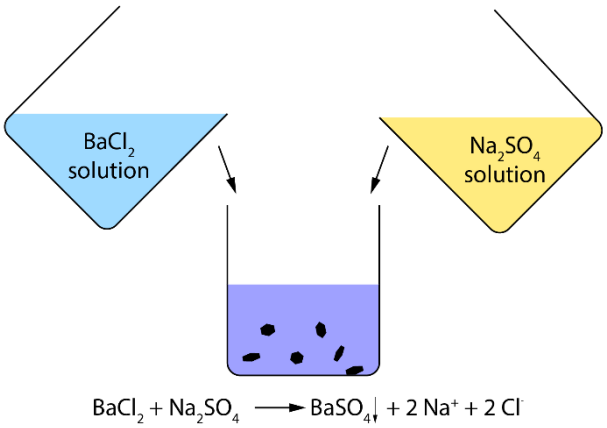

Figure 1: Supersaturation and precipitation through mixing of two solutions.

2.2 Flow-through Experiment

2.2.1 High-Pressure-High-Temperature Apparatus

The high-pressure-high-temperature apparatus shown in fig. 2 consists of three main components: a water reservoir autoclave, a heat exchanger system and a sample autoclave. The fluid is pumped in a closed circuit under geothermal conditions. The flow rate is controlled by a piston-membrane pump (LEWA HUM 1) and can be adjusted between 0.5 to 4.5 g/s. This is monitored by a Coriolis flow meter. The apparatus is designed for temperatures up to 200 °C and pore pressures up to 300 bar. The present setup allows up to 90 °C and 120 bar limited by the heating fluid and current calibration.

The sample autoclave is made of austenitic stainless steel 1.4571, has a usable height of 300 mm and an internal diameter of 100 mm. The water reservoir autoclave is upstream, has a volume of 5 L and is made of austenitic stainless steel 1.4301. In between is a heat exchanger to simulate the heat extraction during geothermal production, i.e., the hot fluid from the reservoir is cooled down, injected into the fractured rock sample located in the sample autoclave and pumped back into the reservoir. To study the influence of specific crystal habits, it is possible to inject a crystal-contaminated suspension through a high-pressure pump (Waters 515 HPLC Pump) after the heat exchanger in front of the sample.

Further components are two digital pressure transducers (WIKA IS-10 with Greisinger GRA 0420 VO) for up- and downstream pressure, an analog manometer, a sampling point, an electrical conductivity meter (AMT Analysemesstechnik), three temperature sensors (thermocouple type K), a gas cylinder to pressurize the system and two smaller autoclaves with a volume of 400 ml each (NWA – New Ways in Analytics). One of them includes a high-pressure-high-temperature pH probe (Pfaudler type 18) and the other one can be used as a saturation container (e.g., be filled with crushed material). Everything is connected through high-pressure pipes (austenitic stainless steel 1.4404) with an inner diameter of 4 mm and multiple ball valves allowing different pathways to in- or exclude some components, e.g., for maintenance.

The temperature is mainly regulated by two thermostats, one each for the water reservoir (Haake N3) and sample autoclave (Julabo F30-HC/6 + 1150 S). In addition, there are two electric heating elements for each smaller autoclave and an electric heating wire along the pipes.

During the experiments, all data (temperature, pressure, flow rate, pH, electric conductivity) can be stored and displayed on a computer with a LabVIEW-system (National Instruments).

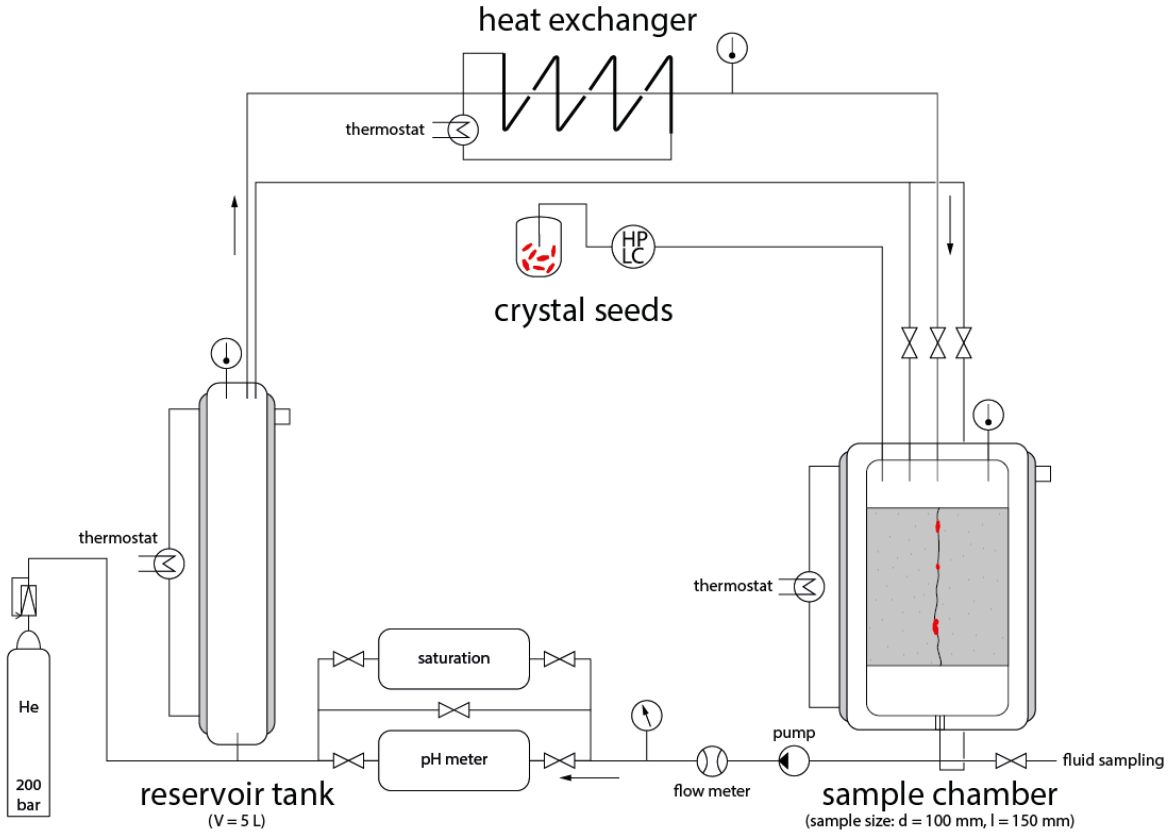

Figure 2: Schematic flow diagram of the high-pressure-high-temperature apparatus which resembles the geothermal production cycle. The fluid flow direction is clockwise as indicated by the arrows.

2.2.2 Rock sample

To study permeability changes in geothermal systems, it is necessary to use fractured samples of reservoir rocks. For this the Flechtinger sandstone was chosen as an analogous of the Groß Schönebeck geothermal reservoir rock (North German Basin). Samples were collected as blocks from a quarry near Bebertal northwest of Magdeburg. From these blocks' cores were drilled with the dimensions of 150 mm length and 99.5 mm diameter. The fracture was induced with a hydraulic press.

The Flechtinger sandstones is red, well-sorted, fine-grained and consist mainly of quartz (63 %), potassium feldspar (18 %) and sodium plagioclase (6 %). It is cemented by phyllosilicates (11 %). Calcite (< 1 %), hematite (< 1 %) and barite (< 1 %) are accessory minerals. The grain density is 2.67 g/cm^3. It is a Lower Permian (Rotliegend) sedimentary rock and cross-bedded, sometimes laminated. The mean grain size is 0.5 mm. The phyllosilicate is mainly illite. The porosity and permeability (not fractured) are 10 ± 1 % and 0.04 ± 0.02 mD (Heiland and Raab, 2001; Hassanzadegan et al., 2012).

2.2.3 Fluid Composition

The fluid is made to be in equilibrium with the rock sample to minimize dissolution effects in the flow-through experiment. Pure water (type II) is mixed with crushed rock material from the same origin as the rock sample in 5 L borosilicate glass flasks on a shaking table at 90 °C for 5 days. It is pressure filtered with a cellulose nitrate filter membrane (pore size 0.45 µm, Sartorius AG) and then filled into the high-pressure-high-temperature apparatus.

2.2.4 Experimental Parameters and Procedure

The fractured rock sample is heat-shrinked into a PTFE shrinking tube with a wall thickness of 0.1 mm, saturated with the same fluid as used in the experiment and then inserted into a sample holder within the sample autoclave. The apparatus is filled with the preconditioned fluid. During the first 24 h the flow rate is set to 4 g/s to quickly heat up the apparatus to about 60 °C. The sample autoclave including the rock sample is not flowed through yet. After 24 h the flow rate is reduced to 3 g/s, a fluid sample is taken, and the sample autoclave valves are opened. Then the pore pressure is raised to 90 bar. For the next 6 days no parameters are changed to achieve equilibrium. On the 7th day another fluid sample is taken. Then 900 ml of a suspension consisting of pure water and 400 mg of barite crystallites from the precipitation experiments are injected at rate of 10 ml/min. After 24 h and another 7 days fluid samples are taken and the experimental run ends (14 days in total).

2.3 Analytics

2.3.1 Sample Preparation

After the experiment, the rock sample is taken out of the apparatus and taken apart along the fracture. One half is stored and the other one is glued along the edge with silicone on another sample holder to prevent damage to the fracture surface in the subsequent preparation steps. These include several cuts to make an approx. 0.5 cm thick plate which is then divided into eighths.

2.3.1 X-ray Powder Diffraction (XRD)

X-ray powder diffraction was used to determine crystallinity and mineral phase of different samples. For this a PANalytical Empyrean X-ray diffractometer was used. The tube (CuKα) was operated at 45 kV and 40 mA. Data were collected from 5 – 80 ° 2θ in step size of 0.026. The samples were ground to fine powders before analyses.

2.3.2 Scanning/Transmission Electron Microscope (SEM/TEM) and Energy-dispersive X-ray Spectroscopy (EDX)

To study the chemistry, size, morphology and distribution of the samples a ZEISS - Gemini2 - Merlin HR-FESEM with a Schottky field emitter was used. It was operated at different voltages and currents (5 - 20 kV, 150 - 1000 pA). The secondary electron (SE) and backscattered electron (BSE) detectors were used for imaging purposes while the energy-dispersive X-ray spectroscopy detector was used to determine the chemical composition of the samples.

For the analysis of the samples from the precipitation experiments a representative piece with enough residue and dimensions of about 2 x 2 mm was cut from the cellulose nitrate membrane filter and glued on to a 5 mm diameter holder with a sticky carbon pad. A few samples were analyzed with a Jeol 2100 - HRTEM (Technical University of Darmstadt).

For the flow-through experiments one eighth of the fracture surface was glued on a 25 mm diameter holder with four carbon pads and carbon paste. All samples were sputtered with 25 nm of Au using a sputter coater (Cressington Turbo Sputter Coater 208HR). Approx. 300 BSE images were taken of one eighth of the fracture surface to distinguish mineral phases.

3. RESULTS AND DISCUSSION

3.1 Precipitation Experiments

Right after mixing barium chloride and sodium sulfate solutions without any other solute the resulting solution becomes cloudy which is a sign of crystallization. The induction time is instant. Furthermore, the crystallization duration (10 s - 30 h) after mixing does not have an impact on crystal size, distribution or morphology. There is bimodal size and morphology distribution. There are rectangular plate-like crystals (fig. 3, first image to the left) with 5 µm x 3 µm and a non-measurable thin thickness (approx. 0.1 µm) as well as smaller roundish agglomerates (2.5 µm diameter) of these plate-like crystals. The concentration of barium chloride and sodium sulfate in the range of 0.4 mmol/L to 0.9 mmol/L does not have a big influence on the size and morphology, too. Only from 1.0 mmol/L a rounding of crystal faces and general enlargement of the crystals is recognizable.

Rising concentrations of sodium and chloride in solution as a background electrolyte shows an inhibition or slowdown of the crystallization process as described in the literature (Canic, 2015; Goulding, 1987). The first turbidity is visible after 10 to 20 minutes depending on the concentration of NaCl. Furthermore, the morphology of barite changes significantly. Fig. 3 shows SEM and TEM images of precipitated barite crystals with 0, 0.1, 0.5 and 1.0 mol/L NaCl (left to right) in solution. The background electrolyte inhibits the growth of specific crystal faces thus changing the crystal morphology. The model shows an inhibition in {001} and {100} – these faces are getting more surface. At 0.5 and 1.0 mmol/L new faces become visible. The crystallite sizes become smaller with the biggest change from 0 to 0.1 mmol/L.

Fig. 4 shows two examples of produced barite crystals with distinctly different morphologies. The crystals pictured on the left side have a planar star-like morphology with a large surface to body ratio while the barites on the right are more like a rounded double-pyramids with a higher bulk mass. The dimensions differ from about 12 µm diameter (star-like) to 4 µm x 2 µm.

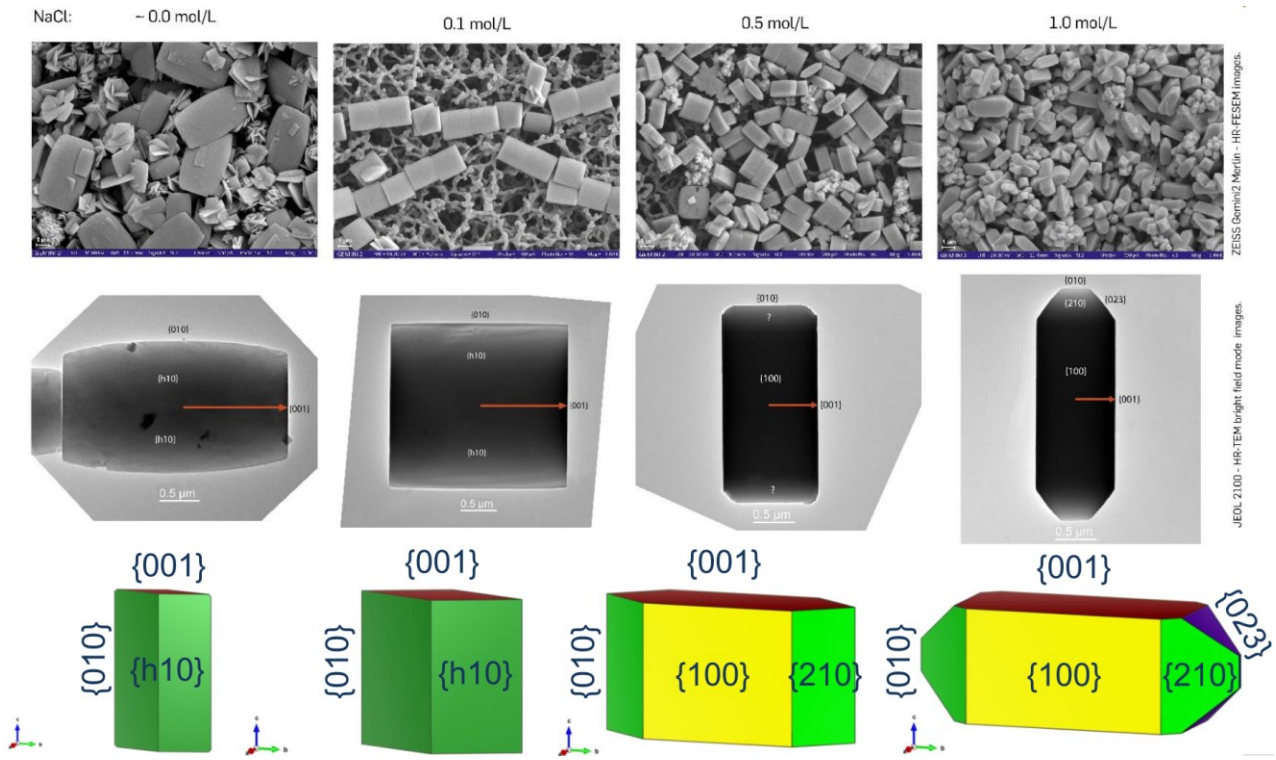

Figure 3: SEM SE images (top) showing the change in barite size and morphology with rising sodium chloride concentrations. TEM field mode images (middle) show higher resolution and indexed crystal faces. Simplified model (bottom) for clarification is made with Vesta (Momma and Izumi, 2011).

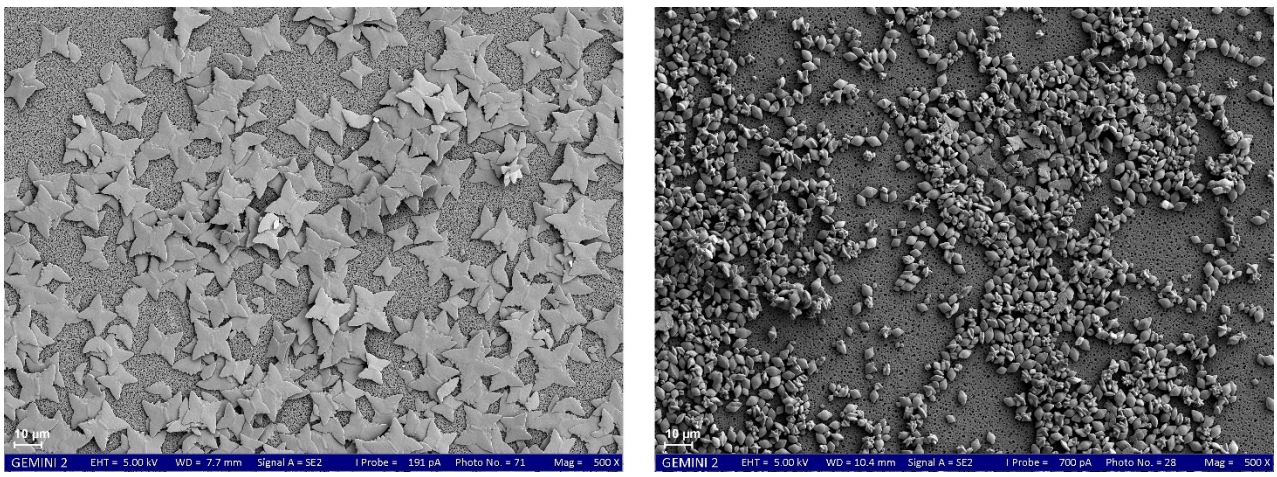

Figure 4: SEM SE images of different barite morphologies. Left: barite crystallized from 2.0 mmol/L barium chloride and sodium sulfate solutions at 65 °C. Right: barite crystallized from 5.0 mmol/L barium chloride and sodium sulfate with 1.0 mol/L NaCl and 0.1 ml/L DTPMP at 23 °C.

3.2 Flow-through Experiment

Initial functionality of the high-pressure-high-temperature apparatus was tested. First flow-through experiments at elevated pressure and temperature conditions were conducted. The LABVIEW data acquisition system is working. The temperature of the water reservoir and sample autoclaves can be kept constant with a precision of 1 °C. The heat exchanger is able to cool down the fluid from 90 to 30 °C with tap water as a cooling fluid (14 °C). The piston-membrane pump circulates the water in the system although some pore pressure (5 bar) is necessary. Furthermore, pressure oscillations of about 2 – 4 bar depending on the flow rate are observed. Pore pressures of up to 120 bar were tested and the apparatus has remained tight.

The whole flow-through experiment lasted 14 days. A fluid sample was taken before the experiment from the preconditioned fluid (2.2.3) and after 1, 7, 8 and 14 days. The flow rate was set to 4 g/s for the first 24 h and then reduced to 3 g/s for the remaining time. Unfortunately, the pump stopped working after 7 days and the flow rate dropped to 0 g/s for 24 h. It was restarted on the 8th day, started again with a flow rate of 3 g/s but dropped to a fluctuating 0 g/s – 1.5 g/s after half an hour for the rest of the experiment. The temperature in the reservoir was approx. 61 °C the whole time. The temperature in the sample autoclave was 59 °C for the first 7 days, increased to 60 °C for 24 h when the flow has stopped and decreased to 58 °C after the flow was reinstated. The temperature at the pH probe followed the same rhythm as the temperature in the sample autoclave but the steps were 58 °C, 66 °C and 56 °C – 58 °C. The pH value increased from 5.6 in the beginning to 6.3 at the end of the experiment.

24 h after the start of the experiment the up- and downstream pressures are approx. 88.3 bar and 87.0 bar resulting in in difference pressure of about 1.3 bar. This value is rising for the next 6 days to approx. 3.4 bar. After the 7th day the fluid sampling leads to a disturbance in the pressure stability. Furthermore, the pump stops working, and the difference pressure drops to 0.5 bar. After restarting the pump, the downstream pressure drops to a fluctuating 3 bar to 10 bar resulting in a pressure difference of approx. 80 bar. It is not clear if the pressure disturbance and malfunctioning of the pump resulted from the fluid sampling or other reasons (e.g., redeposition of loosened particles in the rock sample or pump, electric malfunction of the pump etc.). Nevertheless, during the next experiment there will be no in situ fluid sampling but only before and afterwards in order to exclude it as a problem. After 14 days the rock sample was extracted from the sample autoclave and an outbreak in the bottom part of the sample was discovered. Because of this a deposition tank was added after the sample autoclave to prevent particle accumulation in the pump.

Fig. 5 shows the sandstone fracture surface (left) after the experiment. White residue is widely visible with the eye and proven to be barite by EDX measurements. The stitched panoramic SEM BSE image (top right) is showing the same distribution patterns as the photograph but with much higher detail. The SEM BSE image with a greater magnification is showing the deposited star-like barite crystals as produced and analyzed in precipitation experiments (fig. 4 left) besides larger barite crystals from the original sandstone (as occurring in reference sandstone samples). These deposited barites show no signs of crystal growth or cementation processes. It seems that there is no supersaturation regarding barite. The experimental conditions should be changed to provoke this mechanism (e.g., cooling of the fluid with the heat exchanger in addition to injecting crystallites) to gather more information about growth kinetics of barite in sandstone fractures under geothermal conditions.

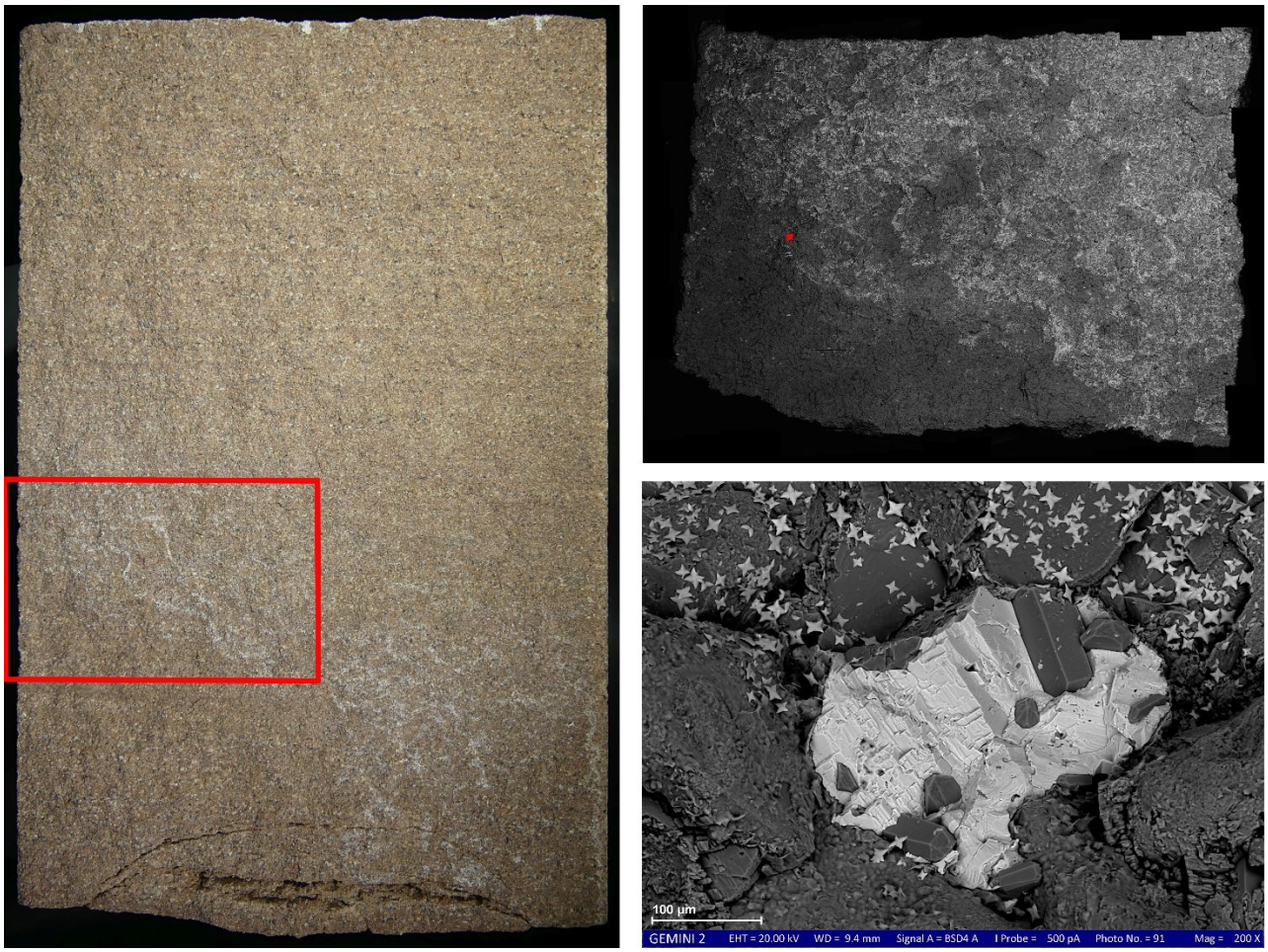

Figure 5: Left: Photograph (approx. 150 mm x 100 mm) of the fracture surface with white barite particles and marked area. Top right: SEM BSE image stitched from about 300 single images (approx. 40 mm x 30 mm) representing marked area from the photograph on the left. Bottom right: SEM BSE image with a much higher magnification (scale bar 100 µm). Large barite crystal in the middle (white) is presumably from original sandstone. Smaller star-like barite crystals are from the injection during the experiment.

Fig. 6 depicts the further workflow based on two exemplary SEM BSE images. One eighth of the fracture surface can be analyzed in the SEM by automating the collection of BSE images (A to B). These images can be stitched to a get high resolution overview of the sample area (B). Barite can be easily distinguished from other mineral phases in the sandstone through the BSE images (B, C and D). Different distributions and deposition patterns are already visible. False color images can help to statistically evaluate the deposited barite crystals.

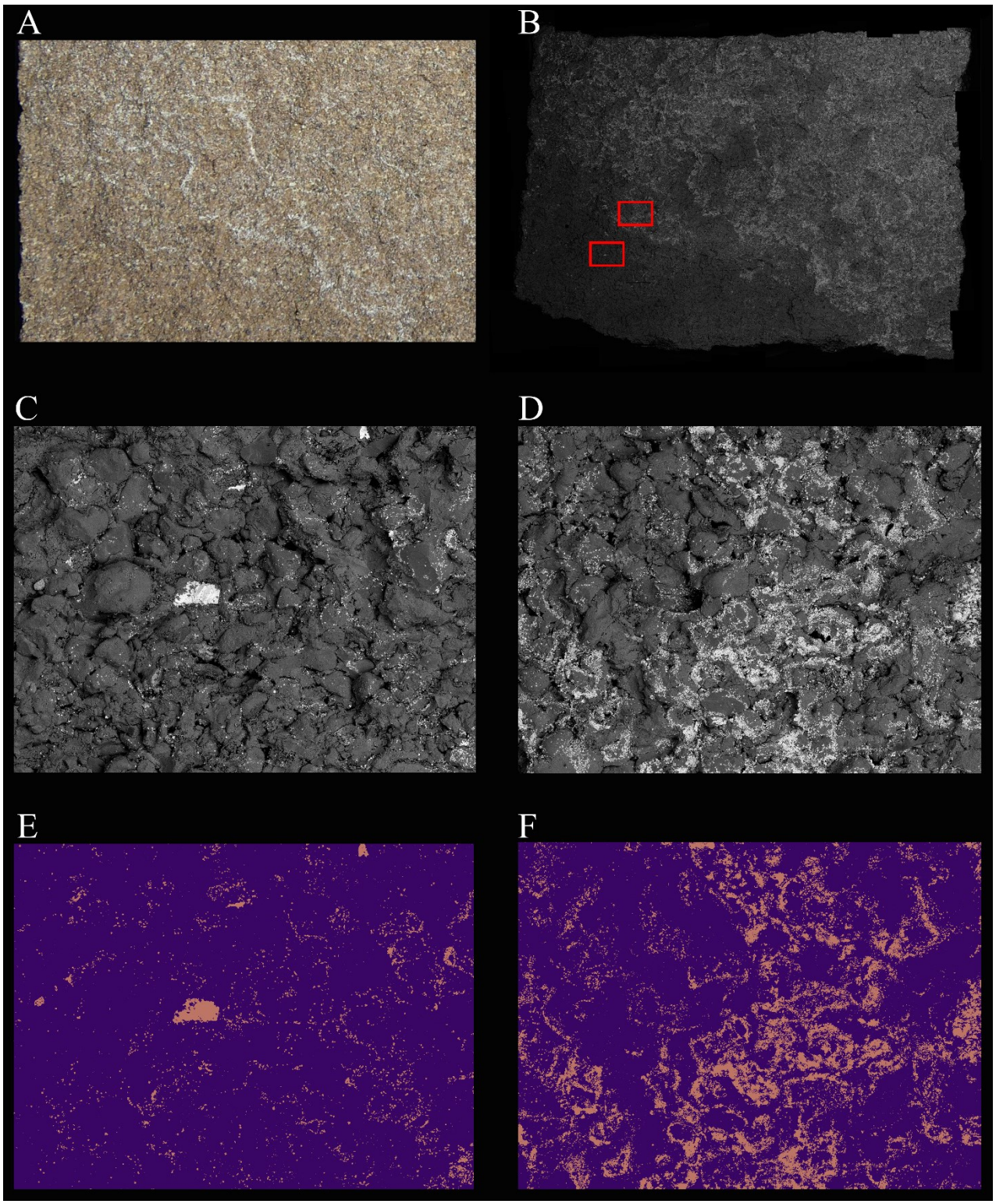

Figure 6: A: Enlarged photograph (approx. 40 mm x 30 mm) of one eighth of the fracture. B: Stitched SEM BSE image (approx. 40 mm x 30 mm) with marked sections (bottom left: C, E; top right: D, F). C, D: SEM BSE images (approx. 3.4 mm x 2.7 mm) with higher magnification from which B is stitched. E, F: False color images to distinguish barite from other minerals (pink: barite; purple: rest of the sandstone).

4. CONCLUSION

The high-pressure-high-temperature apparatus is ready to be used despite of some smaller problems. The main features like controlling temperature and pressure conditions as well as the fluid flow are working. The injection of a suspension with laboratory grown barite crystals, their subsequent deposition in the sandstone fracture and successfully analysis was shown but further evaluation is still necessary. With this setup the filter effects and cementation processes in fractured rocks can be studied. There are many experimental conditions to be investigated and experimental runs to be compared. The revealed problems are already taken care of for the next experimental runs with the mentioned solutions.

5. ACKNOWLEDGEMENT

The authors gratefully acknowledge the financial support of the Federal Ministry for Economic Affairs and Energy (BMWi) managed by Forschungszentrum Jülich. Further we thank our project partners at TU Darmstadt, JGU Mainz, GFZ Potsdam and Geomecon GmbH.

REFERENCES

Blöcher, G., Reinsch, T., Henninges, J., Milsch, H., Regenspurg, S., Kummerow, J., Francke, H., Kranz, S., Saadat, A., Zimmermann, G., and Huenges, E.: Hydraulic history and current state of the deep geothermal reservoir Groß Schönebeck, *Geothermics*, **63**, (2016), 27-43.

Bott, T.R.: *Fouling of heat exchangers*, Elsevier, Amsterdam, (1995).

Canic, T., Baur, S., Bergfeldt, T., and Kuhn, D.; Influences on the barite precipitation from geothermal brines, *Proceed. World Geothermal Congress 2015*, Melbourne, Australia, (2015).

Goulding, P.S., Formation damage arising from barium sulphate scale precipitation. *PhD-Thesis*, Heriot-Watt University, (1987).

Hassanzadegan, A., Blöcher, G., Zimmermann, G., and Milsch, H.: Thermoporoelastic properties of Flechtinger sandstone, *International Journal of Rock Mechanics and Mining Sciences*, **49**, (2012), 94-104.

He, S., Oddo, J.E., and Tomson, M.B.: The Nucleation Kinetics of Barium Sulfate in NaCl Solutions up to 6 m and 90°C, *Journal of Colloid and Interface Science*, **174**, (1995), 319-326.

Heiland, J., and Raab, S.: Experimental investigation of the influence of differential stress on permeability of a lower permian (rotliegend) sandstone deformed in the brittle deformation field, *Physics and Chemistry of the Earth, Part A: Solid Earth and Geodesy*, **26**, (2001), 33-38.

Orywall, P., Drüppel, K., Kuhn, D., Kohl, T., Zimmermann, M., and Eiche, E.: Flow-through experiments on the interaction of sandstone with Ba-rich fluids at geothermal conditions, *Geothermal Energy*, **5**, (2017).

Parkhurst, D.L., and Appelo, C.A.J, Description of input and examples for PHREEQC version 3 - A computer program for speciation, batch-reaction, one-dimensional transport, and inverse geochemical calculations, *U.S. Geological Survey techniques and methods, modeling techniques, groundwater*, Denver, Colorado, U.S. Geological Survey, (2013).

Regenspurg, S., Feldbusch, E., Byrne, J., Deon, F., Driba, D.L., Henninges, J., Kappler, A., Naumann, R., Reinsch, T., and Schubert, C.: Mineral precipitation during production of geothermal fluid from a Permian Rotliegend reservoir, *Geothermics*, **54**, (2015), 122–135.

Scheiber, J., Seibt, A., Birner, J., Genter, A., and Moeckes, W.: Application of a scaling inhibitor system at the geothermal power plant in soultz-sous-Forêts: laboratory and on-Site studies, *Proceedings*, European Geothermal Congress, Pisa, Italy, (2013).

Schuster, V.: Gekoppelte hydromechanische Thermo-Triaxialversuche an Sandsteinproben zur Bestimmung poroelastischer Parameter, *Master Thesis,* TU Darmstadt, (2017).

Shi, W., Kan, A.T., Fan, C., and Tomson, M.B., Solubility of Barite up to 250 °C and 1500 bar in up to 6 m NaCl Solution, *Industrial & Engineering Chemistry Research*, **51**, (2012) , 3119-3128.

Stober, I., and Bucher, K.: *Geothermie*, Springer Spektrum, Berlin, (2014).

Momma, K. and Izumi, F.: VESTA 3 for three-dimensional visualization of crystal, volumetric and morphology data, *J. Appl. Crystallogr.*, **44**, (2011), 1272-1276.

Vidal, J., and Genter, A.: Overview of naturally permeable fractured reservoirs in the central and southern Upper Rhine Graben: Insights from geothermal wells, *Geothermics*, **74**, (2018), 57-73.

Wolfgramm, M., Rauppach, K., and Thorwarth, K.: Mineralneubildung und Partikeltransport im Thermalwasserkreislauf geothermischer Anlagen Deutschland, *Z. geol. Wiss*, **39**, (2011), 3-4.